DEVELOPING A NEW ADDITIVE MANUFACTURING TOOLPATH STRATEGY FOR CONTINUOUS FIBRE COMPOSITES

Tawfik, H.[1]*, Elderfield, N.[1], and Wong, J.[1]
[1] Laboratory of Engineering Materials, University of Calgary, Calgary, Canada
* Corresponding author (hussam.tawfik@ucalgary.ca)

Keywords: *toolpath optimization, continuous fibre fused filament fabrication (CF-FFF), fibre steering*

ABSTRACT

Additive manufacturing of continuous fibre composites requires the development of new tool-pathing algorithms which consider both the anisotropic and continuous nature of the reinforcement material. Up to now, 3D printing slicing software developed for isotropic materials, like neat polymers, have been adapted for continuous fibre composites resulting in a layer-by-layer approach which forces the filaments to be cut after each layer has been deposited. This approach imparts discontinuities in the reinforcement, creating weak points, and does not fully exploit the strength of continuous fibre materials. In this work, a novel approach to tool-pathing is proposed which considers 1) fibre continuity across more than a single layer by allowing for overlapping filaments and 2) strategic positioning of the fibre cut points as determined by the load case and modelled using finite element modelling. This novel tool-pathing approach is demonstrated on a simple geometry characterized by a bracket with two load-application inserts. Finite element analysis is used to model the stress distribution under tensile and compressive loading, where areas under the least stress are identified as suitable cut point regions. The brackets produced using the new tool-pathing algorithm are compared to those manufactured using approaches used by commercially available slicing options. All brackets are tested to failure under tensile and compressive loading and their mechanical performance is reported and compared.

1 INTRODUCTION

Additive manufacturing (AM) of continuous fibre reinforced polymer composites (cFRPCs) presents challenges and opportunities in developing manufacturing toolpaths due to the anisotropic and continuous nature of the reinforcement fibres. Compared to the toolpaths used for isotropic thermoplastic polymer materials, toolpaths used for cFRPCs must consider fibre steering and locations of fibre discontinuities to fully exploit the excellent mechanical properties of cFRPCs. The development of software tools for achieving structurally optimal fibre orientations, maximizing the continuity of fibre paths, and placing fibre discontinuities in minimal stress regions is highly desirable.

Limited research has been reported on optimizing toolpaths for 3D printing of cFRPCs. Groups that have focused on this work mainly aimed to align fibres in stress flow direction [1][2][3]. They developed algorithms for structural components like cantilever and three-point bending beams. Others have used the tool pathing freedoms offered by AM to steer fibres around holes in simple tensile specimens based on stress tensor analysis to reduce stress concentration around holes [4][5][6][7]. Nanya Li et al. [2] additively manufactured a carbon fiber-nylon composite plate by steering fibres along load transmission paths around holes. This fibre steering was shown to improve tensile and flexural strength 67.5% and 62.4% respectively when compared to samples where holes were drilled, creating discontinuous fibres. K. Sugiyama et al. [4] steered fibres along the principal stress direction around a hole. Replacing the unidirectional plies in a laminate with the optimized plies increased stiffness 9.4 times. Wang et al. [1] developed a Stress Vector Tracing algorithm to generate load-dependent printing paths for cantilever structures. Papapetrou et al. [3] implemented different topology and morphology methods to align fibres along principal stress trajectories. Most of the existing research optimizes toolpaths for generic structural components like composite plates containing holes, cantilever beams, and simply supported beams.

Herein, we demonstrate the impact of strategically selecting the location of cut points and maximizing the continuity of fibres on an additively manufactured structure through a simple case study geometry. A simple bracket with two load application points as shown in Figure 1a is selected. The bracket consists of two circular structures with diameters of 45 mm and a center-to-center separation of 100 mm, connected by two straight profiles. Finite element modelling (FEM) is used to determine the location of highest and lowest stresses under tensile (Figure 1b) and compressive loads. The brackets were manufactured using different toolpath strategies (Figure 1c and d) comprising two conventional slicing methods and one toolpath optimized for cut points and fibre continuity. The specimens were mechanically tested (Figure 1e) and compared.

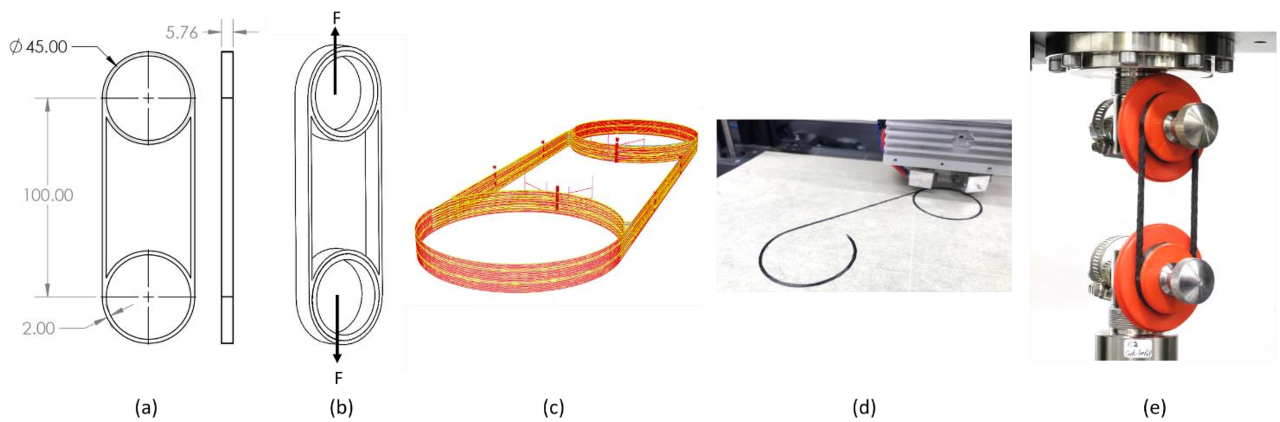

Figure 1. Simple bracket structure. (a) Specimen dimensions in mm. (b) Isometric view and force direction under tensile loading. (c) Tool path visualization. (d) 3D printing of the specimen. (e) Manufactured specimen in testing setup.

2 FEM analysis for strategic cut point placement (SCPP)

Finite element modeling (FEM) analysis was performed to determine stress distribution and locate areas of minimum and maximum stress within the structure under tensile (Figure 2a) and compressive (Figure 2b) loading conditions. The objective here was to identify locations where discontinuities caused by cut fibres would result in minimal loss in mechanical performance (i.e., locations of minimum stress). The structure was modeled using a generic anisotropic carbon fibre-reinforced material in Altair HyperWorks 2021, with Young's moduli of 140 GPa and 12 GPa in the directions parallel and transverse to the fibres, respectively. The fibre orientation for each mesh element was defined to be parallel to the direction of material deposition (circumferentially aligned in the circular sections and longitudinally aligned in the straight sections). A single layer was simulated with a width of 2 mm and thickness of 0.3 mm. Full width mesh elements with an approximate 1:1 aspect ratio were used to represent the geometry. Fixed and load application points were defined to mimic the physical test setup, whereby only the interior facing edges of the circular sections were fixed or loaded for the tensile analysis (Figure 2a), and only the exterior facing edges of the circular sections for tensile loading (Figure 2b).

The resulting stress distributions are illustrated in Figure 2c and d. Different regions were classified according to the corresponding stress concentration magnitude and listed from least to most critical. In both load cases, the inner and outer arcs of the circular sections have the lowest stress concentrations. The transition regions between the circular and linear sections show the highest stress values.

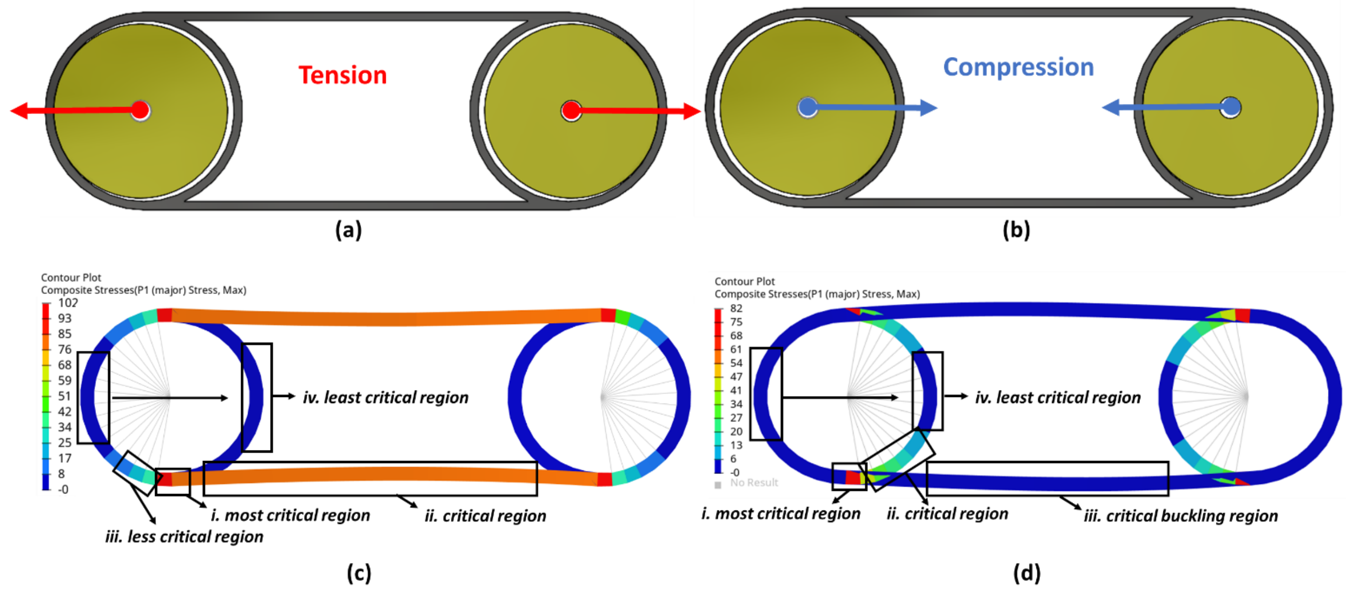

Figure 2. FEM simulation results for the structure under tensile and compression loading. Test setup schematic for (a) tension and (b) compression. Stress distribution for (c) tension and (d) compression load cases.

These simulation results are consistent with literature. Several reports on loop structure failure confirm that the transition of the loop from contact with the fixture insert to the straight strand is the most critical region (Region *i* in Figures 2c and 2d), where failure-triggering stress peaks occur. The sections of the loop in contact with the insert are subjected to internal pressure, which results in a tensile strain in the outer section over the thickness. However, the inner radius is constant and is determined by the insert's radius. As the outer section is stretched over the thickness, while the inner section is constant, a bending moment is induced. This results in a stress distribution of superimposed tensile stress at the outer radius and compressive stress at the inner radius [8]. The straight regions which connect the loading points are categorized as region *ii* and are critical for bearing the tensile loads. On the other hand, regions *iii* and *iv* in Figure 2c are less critical to failure. Region *iv* may fail under compression at the insert, and region *iii* may fail due to shear stresses [9].

Under compression loading, the straight section of the oblong (region *iii* in Figure 2d) is subjected to buckling. Region *i* with the highest stress concentration values acts as a fixed connection at the end of the buckling column and is subjected to bending stresses. Similar to the tensile loading case, regions *ii* and *iv* in Figure 2d will fail under compressive and torsional stress, respectively. Accordingly, regions *i*, *ii*, and *iii* are considered as "no cut" regions. During toolpath planning, it is preferable to cut fibres only at region *iv*, where mainly compressive stresses apply.

2.1 Toolpath planning

2.1.1 Conventional toolpaths based on slicing method

In conventional 3D printing slicing algorithms, toolpaths are strictly two-dimensional, meaning that it is not possible for a toolpath to step up from level to another without a discontinuity in the filament (an exception being "vase mode" type algorithms used in polymer slicers). To deposit material in the form of the bracket in this case study, four fibre layout variants are possible. Figure 3 shows a top view of one layer of each variant. The first layout variant is an oblong that starts and ends with cut points in the least stressed regions (see Figure 3a), followed by two inner arcs to realize the loop's circles. It is obvious that this variant is useless for compression since the internal arcs are not attached to the structure by continuous fibres. However, it may perform well under tensile if the cut location (i.e., weak point) in the oblong alternates in each successive layer, as shown in Figure 3e. The second variant is a 96 layout. By alternating the layout from a "96" to a "Pd"-like shape (see Figure 3f), the weak points will be evenly distributed among the structure. This variant is considered a good compromise for both tension and compression load cases. Accordingly, Specimen "96-Pd" (see Figure 3f) was tested under both tension and compression. While specimen "outer oblong" (see Figure 3e) was tested under tension only.

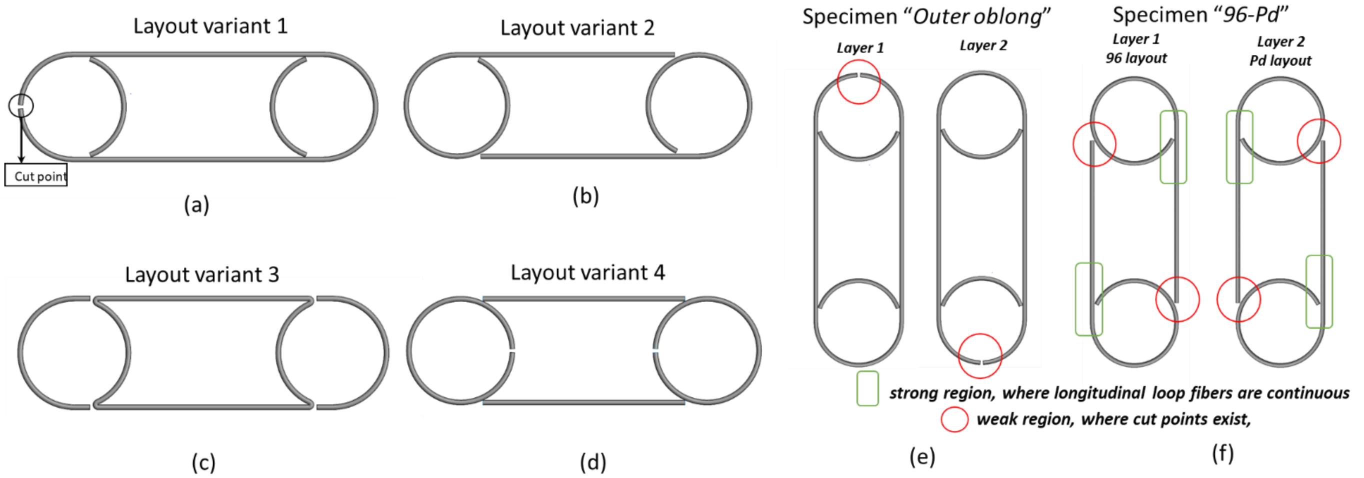

Figure 3. Fibre toolpath using the slicing method: (a) Proposed layouts. (b) Top view of the selected layouts, showing cut point alternating in each successive layer.

Layout variants 3 and 4 were not selected to be manufactured because of lack of continuous fibre between load application points which would result in poor mechanical performance. Moreover, both layouts have cut points at the most critical stress region, according to the previous FEM analysis.

2.1.2 Optimized toolpath using Multi-Layer Continuous Fibre Paths (ML-CFP)

Optimizing the tool path using the Multi-Layer Continuous Fibre Path (ML-CFP) strategy means strategically positioning cut points and minimizing the number of cut points in a build volume. For the bracket used in this case study, two toolpath layouts were designed for optimized performance in tension and compression. According to the FEM simulation, cut points (i.e., loop start and end points) were located at the inner arcs of the loop. For the compression load case, first, an outer continuous loop is used to connect both the load application points (in grey in Figure 4a), directly followed by an internal loop with no fibre cut in-between. The internal loop is expected to support the structure under compression. For the tensile load case, the inner compression loop was replaced by individual patches of cut fibres to adjust the height at internal arcs and straight lines. The toolpath in Figure 4. (left) can print the whole component in one shot with zero fibre cuts by merging the start and end points. However, doing the same in toolpath in Figure 4. (right), will keep adding more fibre tows on the outer arcs of the oblong, resulting in uneven component height. Therefore, between each continuous loop, four patches of fibre tows are printed to adjust height. Additional fibre patches are more beneficial for tensile samples than inner loops as they replace the sharp fibre turning angle with straight fibre tow.

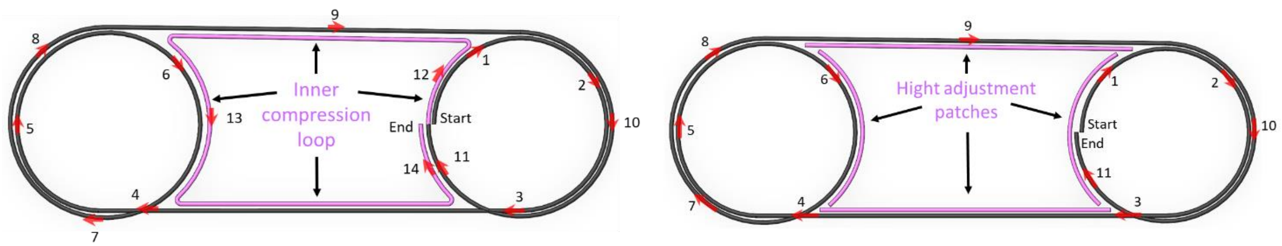

Figure 4. Fibre toolpath using Multi-Layer Continuous Fibre Path (ML-CFP) method. Layout for compression specimens “ML-CFP C” with inner compression loop (left). Layout for tension specimens “ML-CFP T”

3 Experimental Methods

3.1 Fabrication of Specimens

Bracket structures were fabricated on an in-house made custom additive manufacturing system using preimpregnated carbon fibre/PA12 filaments with an approximate fibre volume content of 50% (Apollo CFRP, 9T Labs AG, Switzerland). Specimens were manufactured at room temperature and a ~30% humidity level. Each specimen was manufactured out of 18 layers of 0.32 mm thickness each, providing a total height 5.76 mm. Specimens weighed 26.5 ± 2.3 g. To focus on the effect of fibre toolpath as an initial study, only a single fibre tow was used to give a beam width of approximately 1.6 mm. The printed object was used as formed with no further consolidation.

Toolpaths were planned and g-codes were generated in a custom interface using Grasshopper 3D parametric modeling software. Figure 1c shows a visualization of the toolpath planned for the ML-CFP specimen. 3D printing parameters like the alternating start and end points and programmed cutter actuation positions are visualized.

3.2 Mechanical testing

All specimens were tested at room temperature using a Zwick/Roell Z30 universal testing machine with a 2 mm/min loading rate. Loads were applied to the circular sections using 3D printed polylactic acid (PLA) inserts (manufactured with 100% infill) as shown in Figure 1e. Table 1 shows the list of tested specimens (each with 3-4 identical prints). Results of all tested prints were considered in force values and standard deviations were calculated. The resulting breaking forces (N) and work to fracture (Nmm) were measured using Zwick/Roell testXpert® III software.

Table 1. Tested specimens with different toolpaths under tension and compression.

Toolpath method	Load case	
	Tension	Compression
ML-CFP method	Continuous loop with height adjusting patches “ML-CFP T” in Figure 4 (right).	Continuous outer loop with inner compression loop “ML-CFP C” in Figure 4 (left).
Slicing method	“Outer oblong” in Figure 3e. “96-Pd” in Figure 3f.	“96-Pd” in Figure 3f.

4 RESULTS AND DISCUSSION

4.1 Printing quality

4.1.1 Using the slicing method

Design using the slicing method does not allow fibres to extend outside of a single planar layer. Thus, it required at least 2 cuts per layer to manufacture the simple bracket structure. A total of 36 cuts were used to manufacture the 5.76 mm high part (of 18 layers) which caused several printing feasibility and quality issues like: 1) accumulation of cut fibre frays that resulted in clogging of the nozzle and jamming, 2) regions of uneven fibre tension, since the fibre cut length loses tension after cutting due to detachment from the feed system, and 3) uneven component height due to overlapping or separations at cut ends and new paths' start regions (see Figure 5). To avoid the concentration of the above-mentioned quality defects in a specific location of the structure, the "cut points alternate over each successive layer by rotating the toolpath layout 180° around the center of the component (see Figure 6a).

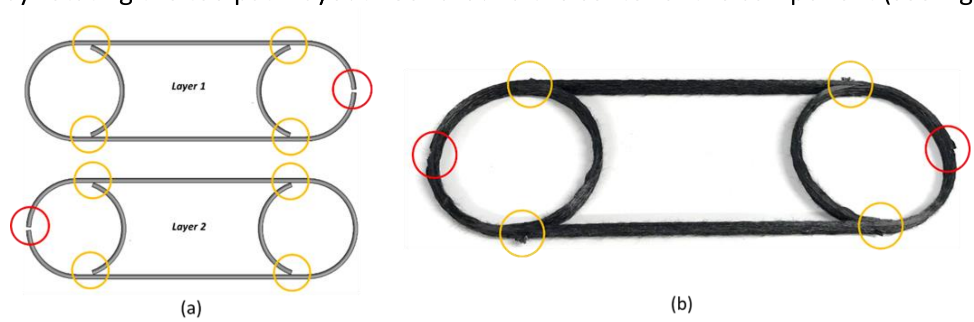

Figure 5. Printing quality issues in the "Outer oblong" specimen using slicing method. (a) Toolpath layout of two successive layers, showing the distribution of cut points. (b) Uneven specimen height, separation, and fibre frays at cut locations.

4.1.2 Using the Multi-Layer Continuous Fibre Path (ML-CFP) method

Printing using the ML-CFP method reduced the number of "cut points" significantly. In ideal design and manufacturing situations the ML-CFP method can reduce the fibre cut count to zero by building the component in single path with only one start and end point. This approach was examined in early AM trials to print the compression specimen shown in Figure 4 (left). The end point of the first printed loop was merged with the successive loop with no fibre cut. Theoretically, the entirety of the compression specimen could have been printed in a single pass without cutting the fibre at intermediate points. However, due to poor fibre tensioning in the print head, filament material kept building up, causing jamming issues at the nozzle and the cutting mechanism after two successive loops. Therefore, the number of loops printed continuously was reduced to one 2-layer tool path. Since one loop of the ML-CFP realizes 2 layers of connected continuous fibres, only 9 cuts (one per 2 connected continuous layers) were required to build 18 layers. "Cut point" locations were alternated over successive layers by rotating the layout 180° to avoid weak regions, as shown in Figure 6a. In future work, the nozzle geometry and feed roller system will be redesigned to compensate for fibre tension build-up to enable printing of the part with one continuous fibre strand.

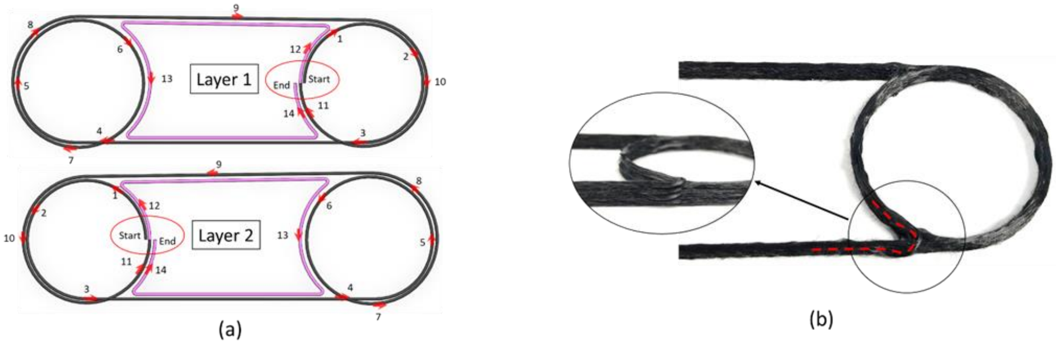

Figure 6. Printing quality of the ML-CFP compression specimen. (a) Toolpath layout of two successive layers, showing the alternating start and end points (cut points). (b) Fibre folding at sharp turning angle of the inner compression loop.

The internal loop, illustrated in pink in Figure 4 (left), was designed with a corner radius of 1 mm. However, due to nozzle tip tolerance and the sharp turning angle of 135°, fibres twist and fold at bigger radius of approximately 2-2.5 mm, as shown in Figure 6b. According to Zhang, Chen, et al., such path deviation is expected for path turning angles >120° and curvature radius <5 mm [13].

4.2 Mechanical Performance

Simple bracket structures manufactured by Multi-Layer Continuous Fibre Path (ML-CFP) showed improvement in mechanical properties (see Figure 7a and b). ML-CFP method tensile specimens fractured at 3.7 kN on average, showing 13% improvement in breaking force over specimen “Outer oblong” that failed at 3.2 kN and 48% improvement over specimen “96-Pd” that failed at 1.9 kN on average. All specimens showed relatively high standard deviations. This large standard deviation is attributed to inconsistencies in the manufacturing process, namely poor interlaminar adhesion. However, the ML-CFP tool pathing method, whose core strength is in connecting different layers together for an even force transmission in the whole component over its thickness, managed to show improvement in breaking forces and work to fracture despite the poor interlaminar adhesion. Enhancing interlaminar adhesion by in-situ compaction or post- 3D printing compaction like compression molding is expected to efficiently illustrate the effectiveness of the Multi-Layer Continuous Fibre Path (ML-CFP) in future work.

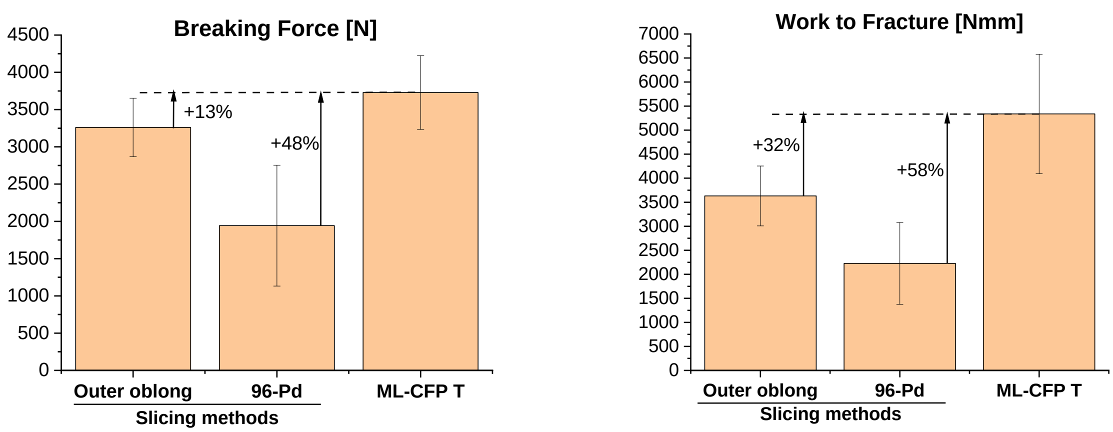

Figure 7. Tensile tests results for different fibre toolpaths. Breaking force (left). Work to fracture (right)

Simple bracket structures manufactured by Multi-Layer Continuous Fibre Path (ML-CFP) method showed significant improvement in work to fracture values. Work done to fracture ML-CFP specimens was 5336 Nmm on average, 32%

and 58% higher than the “Outer oblong” and “96-Pd” respectively, as shown in Figure 7b. Figure 8 shows the failure modes for tested specimens.

Specimen “96-Pd” provided the least work to fracture and break force values. It failed at the start and end points of the 96 and Pd layouts, at the transition of the loop from contact with the fixation inserts. Failure at this location is expected as it witnesses a peak in stress concentration (see Figure 2c). Specimen “Outer oblong” showed intermediate mechanical properties, failing at a non-critical region according to the FEM simulation. It failed at the start and end location of the arc section of the oblong. Specimen “Outer oblong” results illustrate the disadvantage of cut points, that can cause failure at cut points prior to critical regions. While specimen “96-Pd” results show the worst case, when cut points are located at the peak stress concentration regions. Both results conclude the poor utilization of continuous fibres in the structure using the conventional slicing method for tool pathing.

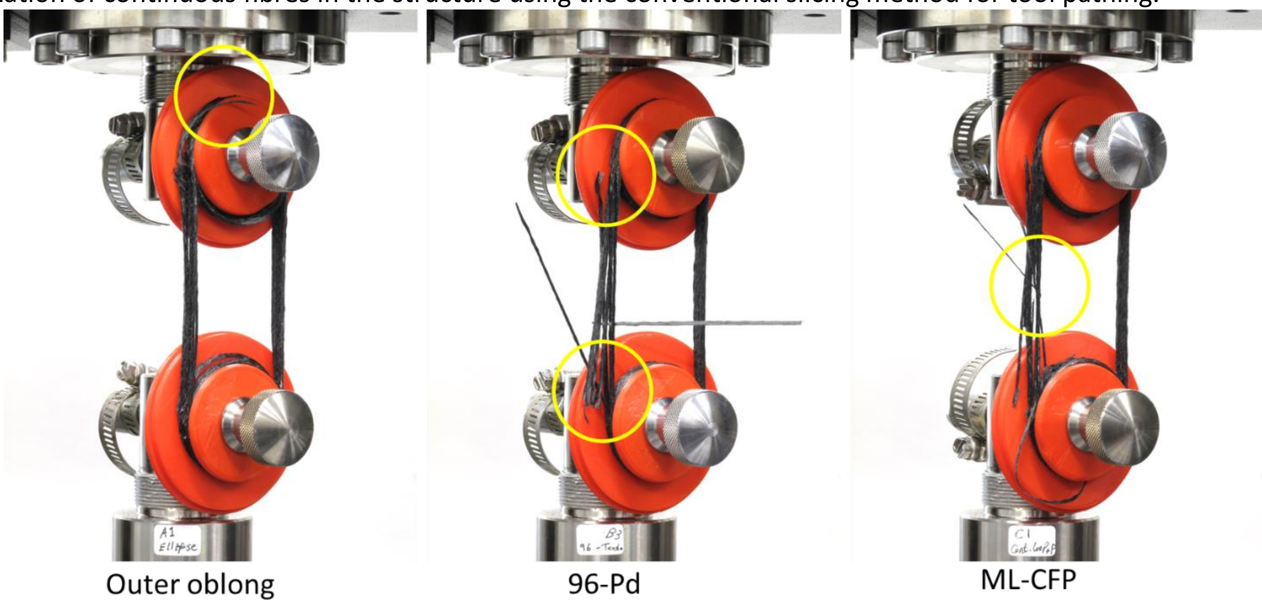

Figure 8. Tensile test failure modes for specimens printed with different toolpaths.

The ML-CFP method specimen eliminated the problem of stress concertation peaks at cut points. With fewer cut points strategically located at the least stressed region (a region with compressive stresses, shown in Figure 2c), the ML-CFP toolpath guaranteed fibre continuity at highest stress concentration regions. Thus, failure occurred either at the middle of the straight section of the oblong (ideal case) or at the transition of the loop from contact with the fixture inserts (where highest stress concertation applies, illustrated in Figure 2c) which indicate better use of the fibres’ mechanical properties. Besides, the ML-CFP method enhances the interlaminar bonding of layers by connecting different layers with continuous fibre. As a result, forces are transmitting evenly along the loop structure’s perimeter and height, and thus, work needed to fracture increased.

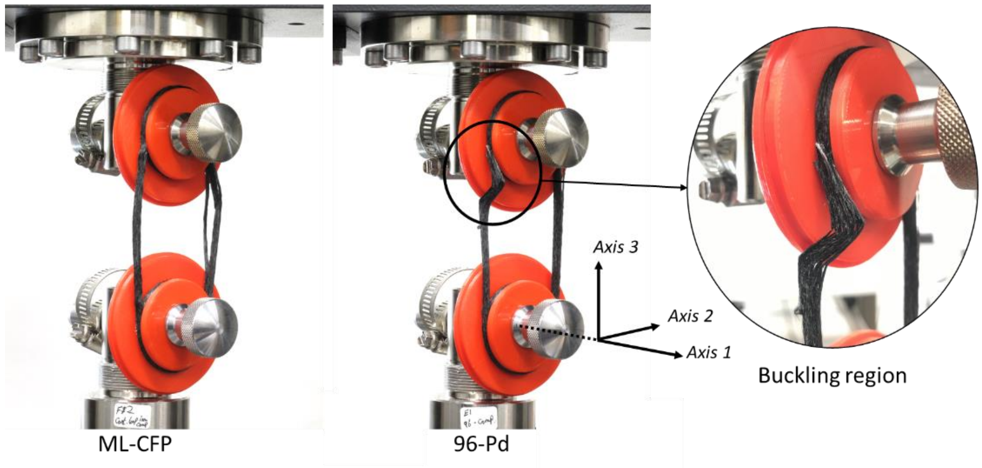

Figure 9. Compression test failure modes for specimens printed with different toolpaths.

Compression samples did not show promising results. Buckling forces for either the “96-Pd” specimen and ML-CFP compression specimen (Continuous outer loop with inner compression loop) did not exceed 150 N. Figure 9 shows failure modes under compression. It is obvious that delamination due to poor interlaminar bonding decreased buckling forces dramatically. Specimens did not buckle around the buckling axis of the oblong’s straight line (illustrated by axis 1 in Figure 9b) as expected. Rather, bucking occurred in the direction of the specimen thickness. This is strong indication that the fibre layers are poorly bonded, and thus act individually to provide higher slenderness ratio than that of the designed thickness (of 5.76 mm). As a result, buckling of the straight profiles occurred around axis 2 instead of axis 1 (Figure 9).

5 CONCLUSION AND FUTURE WORK

A new toolpath planning method was introduced for 3D printing of continuous fibres. The Multi-Layer Continuous Fibre Path (ML-CFP) increases the efficiency of continuous fibres in 3D printed structural; components by 1) reducing the number of fibre cut locations, 2) implementing a strategic cut point placement (SCPP) at the least stressed regions, and 3) enabling continuous fibres to extend beyond a single layer. Mechanical investigations showed improvement in force transmission through the component. Break force and work to fracture improved by up to 48% and 58% respectively for the tension load case, compared to other parts manufactured by the slicing method. Specimens manufactured using the ML-CFP method reduced the number of cut points significantly, and thus, resulted in less stress concentration peaks, better print quality, and less jamming issues during 3D printing. Tensile specimens of the ML-CFP method fractured at the middle of the oblong’s straight section. This failure mode is considered ideal compared to the slicing method specimens, which failed at cut points.

Compression failure modes illustrated the significantly poor interlaminar bonding between printed layers. In future work, interlaminar bonding will be improved by either in-situ compaction or post-printing compaction (like compression molding) of specimens. Furthermore, the ML-CFP will be developed for more complex structures. An algorithm will be developed to automatically plan and generate the toolpath. First, the structure will be a topology optimized for complex load cases and with load application points as fixed design variables. Second, the resulting truss-like structure will be used as a base layout to plan a continuous fibre path that connects all load application points together in one single loop (if possible) or using the least number of distinctive loops. Third, an FEM analysis will be carried out to determine the least stressed regions, where cut points will be located. Finally, the developed algorithm will design the toolpath and automatically generate the G-code for 3D printing.

6 Acknowledgment

This research was supported by a joint Alberta Innovates and NSERC Advance grant, and an NSERC Discovery grant. Hussam Tawfik would also like to thank Antje Graupe Pryor Foundation for funding through the Werner Graupe International Fellowships in Engineering and the Canadian Energy Pipeline Association (CEPA) for support through the Patrick Smyth Graduate Scholarship.

7 REFERENCES

[1] T. Wang *et al.*, “Load-dependent path planning method for 3D printing of continuous fibre reinforced plastics,” *Compos. Part A Appl. Sci. Manuf.*, vol. 140, no. August 2020, 2021, doi: 10.1016/j.compositesa.2020.106181.

[2] N. Li *et al.*, “Path-designed 3D printing for topological optimized continuous carbon fibre reinforced composite structures,” *Compos. Part B Eng.*, vol. 182, p. 107612, Feb. 2020, doi: 10.1016/j.compositesb.2019.107612.

[3] V. S. Papapetrou, C. Patel, and A. Y. Tamijani, “Stiffness-based optimization framework for the topology and fibre paths of continuous fibre composites,” *Compos. Part B Eng.*, vol. 183, no. December 2019, p. 107681, 2020, doi: 10.1016/j.compositesb.2019.107681.

[4] K. Sugiyama *et al.*, “3D printing of optimized composites with variable fibre volume fraction and stiffness using continuous fibre,” *Compos. Sci. Technol.*, vol. 186, no. August 2019, p. 107905, 2020, doi: 10.1016/j.compscitech.2019.107905.

[5] H. Zhang *et al.*, “Failure analysis of 3D printed woven composite plates with holes under tensile and shear loading,” *Compos. Part B Eng.*, vol. 186, no. April, 2020, doi: 10.1016/j.compositesb.2020.107835.

[6] A. N. Dickson and D. P. Dowling, “Enhancing the bearing strength of woven carbon fibre thermoplastic composites through additive manufacturing,” *Compos. Struct.*, vol. 212, no. January, pp. 381–388, 2019, doi: 10.1016/j.compstruct.2019.01.050.

[7] S. H. R. Sanei, A. Arndt, and R. Doles, “Open hole tensile testing of 3D printed continuous carbon fibre reinforced composites,” *J. Compos. Mater.*, vol. 54, no. 20, pp. 2687–2695, 2020, doi: 10.1177/0021998320902510.

[8] H. Schürmann, *Konstruieren Mit Faser-Kunststoff-Verbunden (2nd)*. 2008.

[9] L. K. T. Botzkowski , S. Galkin , S. Wagner , S. P. Sikora, “Experimental and numerical analysis of bolt-loaded open-hole laminates reinforced by winded carbon rovings.,” *Karlsruhe Inst. Technol. (KIT), Inst. Veh. Syst. Technol. Karlsruhe, Ger.*